

Weld Seam Identification Using Edge Detection in Machine Vision

Chenlei ZHAO, Dong WU, Lin XI, Lihong GUO*, Shenghong WU, Xiao LUO, Shunyang HU, Yiran DING

Abstract: In intelligent welding, achieving the automation of weld quality inspection is a significant challenge, and weld seam marking is of crucial importance. For this purpose, a method based on edge detection using binary image preprocessing was developed on the MATLAB platform. Compared with the traditional multi-sensor fusion approach, this method does not require complex sensor integration, simplifying the implementation process. Compared with neural network methods, it is more flexible and simpler. The method first preprocesses the image into a binary image and then compares the weld seam feature marking with the Roberts, Prewitt, Sobel, and Canny operators. The results show that the Canny operator demonstrates a significant performance advantage in the comparison of four indicators: point sharpness, entropy, average gradient, and Quality Assessment of Blended Features. Its performance is 3 to 25 times that of other operators, and it performs best in weld seam feature texture detection, showing high robustness.

Key words: edge detection; grayscale conversion; machine vision technology; weld seam marking

1 INTRODUCTION

In the realm of industrial production, traditional manual visual inspection is both time-consuming and costly. It has become increasingly common to replace human quality inspections with machine vision technology. Computer vision (CV) algorithms can facilitate the full automation of certain visual inspection processes [1]. Application areas include workpiece shape and size quality inspection, surface quality inspection, and impurity detection [2, 3], among others. By constructing a machine vision system on the production line for real-time image acquisition and converting these images into digital signals transmitted to the industrial control system, the system extracts and matches target state features with predefined templates to determine product quality compliance [4]. For automatic welding robots, one of the critical challenges in efficiently and safely assessing the quality of the weld surface lies in addressing the issue of post-weld seam feature marking. This represents one of the key difficulties in the current field of automation for welded components. The prevailing research direction involves developing specialized visual inspection systems based on deep learning and artificial neural networks [5, 6]. Most previous work has relied on neural networks or multi-sensor fusion, which are effective but time-consuming to implement and unsuitable for small-batch manufacturing. This study addresses this gap by evaluating traditional edge detection operators as a simpler, flexible, and more cost-effective solution.

This study focuses on operation scenarios involving small welding batches and the challenges associated with standardizing manual quality inspections. By leveraging machine vision technology, the morphological characteristics of weld seams are accurately identified and marked, enabling subsequent inspection of welding quality after robotic welding. The primary contributions of this study are as follows: (1) The application of traditional image processing techniques to weld seam marking provides a more efficient and concise solution for automating welding quality inspections. Compared to methods utilizing artificial neural networks for weld marking, this approach demonstrates greater flexibility and broader applicability, making it particularly suitable for

small-batch, non-standardized production operations. (2) A visual simulation platform was developed using MATLAB software. This platform facilitates the preprocessing of weld seam graphics post-welding and enables the selection of optimal methods to enhance image quality, thereby simulating weld seam marking. (3) A comparative analysis was conducted among mainstream edge detection algorithms, including Sobel, Roberts, Prewitt, and Canny operators [7]. Through experimental data analysis, the strengths and weaknesses of each algorithm were evaluated, leading to the determination of the most appropriate weld feature marking method for achieving the research objectives of this study.

2 LITERATURE REVIEW

In the inspection of welding quality, numerous studies have been conducted on the characteristic marking of weld seams. The traditional approach involves integrating various sensors to establish a detection system for identifying weld seam features. For instance, Min et al. [8] achieved the identification of weld seam features by processing images through laser contour recognition feature points using a structured light vision inspection system. Experimental results demonstrated the significance of the online quality inspection system in enhancing the production efficiency and qualification rate of welded panels. Additionally, a post-detection system was developed for calculating and detecting weld geometric parameters and defects in laser welding of split-welded blanks. Society et al. [9] aimed to enhance the level of welding automation in the industry. They utilized binocular vision equipment and image processing algorithms to obtain binocular imaging information, which effectively extracted and linked the processed molten pool image information with weld parameters, enabling reasonable control of welding quality. Zeng et al. [10] introduced an innovative non-destructive testing method based on optical fiber sensing by establishing the relationship between signal changes in optical fiber sensors and weld seam characteristics during the welding process. This method exhibits excellent universality across different welding parameters and materials. Moreover, variations in signal vibration can accurately predict the occurrence of

expulsion. Kim et al. [11] used ultrasonic inspection to evaluate fusion weld seams in thermoplastic materials, which strongly attenuate ultrasonic signals, enhancing test sensitivity. In addition, the semi-analytical finite element (SAFE) method was utilized to compare the characteristic guided wave (FGW) modes in plate welded joints. By combining experimental and numerical methods, the sensitivity of different CFGW modes to defects and the energy flow distribution across the cross-section of the circumferential welded joint were investigated. This system has the potential for remote screening of welding defects [12].

Traditional edge detection algorithms are also widely applied in the industrial field for defect detection. Zhai et al. [13] adopted the Canny edge detection operator to achieve three-dimensional non-destructive location of delamination and other defects in glass fiber reinforced polymer (GFRP) laminates. Compared with the commonly used frequency wavelet domain deconvolution method or previous sparse deconvolution methods, it successfully identified the thickness information of the resin layer and achieved lower noise sensitivity. It has obvious advantages in the three-dimensional location and quantitative characterization of layer thickness of delamination defects in GFRP laminates. Wu et al. [14] proposed a novel edge detection framework for automatic milling of aircraft skins in aviation manufacturing to improve the accuracy of aircraft skin milling. By using an edge probability detector based on spatial tangent continuity, it provides the necessary reference; combined with a hierarchical branch search method, the required milling edges are stripped from the original point cloud layer by layer, achieving the generation of the main branches of the edge contour, branch expansion, and branch pruning. Zhou et al. [15] addressed the issue that the existing visual measurement methods for pick-and-place machines focus on specific SMDs. They proposed an automatic and universal method for measuring the parameters of rectangular-pin SMDs with sub-pixel accuracy, where pixel line pairs are refined to the sub-pixel level. Experimental results on a surface mount hardware platform with different components under various angles and lighting conditions demonstrate that the proposed method is highly accurate and robust.

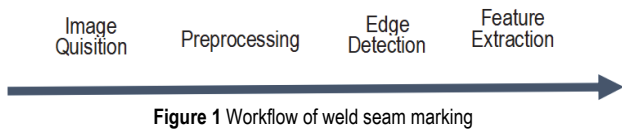
In addition, the edge detection algorithm has also been applied to other engineering fields. Lan et al. [16] proposed an enhanced lane recognition method to address the potential damage to automatic cruise control caused by lane interference, uneven lighting, and darkness at night. They used Canny edge detection to automatically place roadside warning signs. Experiments showed that the proposed technique achieved a lane recognition accuracy rate of up to 85%, outperforming previous threshold methods. By overcoming the shortcomings of lane detection, this study enables reliable automatic deployment of warning signs, thereby enhancing road safety. Wu et al. [17] aimed to address the low level of automation in the process of bridge disease detection and the limitations of traditional image segmentation methods, such as insufficient denoising effect and poor continuity in crack segmentation. By conducting meticulous preprocessing and image segmentation on bridge disease images, they identified and extracted the key features of cracks to enhance the ability to recognize cracks.

3 DETECTION AND PRINCIPLE OF WELD MARKING BY MACHINE VISION

Machine vision is the use of machines to replace human eyes in measuring and judging objects. Machine vision technology is an emerging discipline that integrates multiple fields such as optics, electronics, information theory, and computer science. It is mainly used for detecting surface features or defects of objects, recognizing moving objects, and conducting automated production control. It can simulate the human visual process with computers for automatic control. In the field of industrial control, machine vision is mainly applied to the detection of workpiece dimensions, shape recognition, quality monitoring, etc. A machine vision system converts the captured object into an image signal, which is then sent to a dedicated image processing system. Based on the relationship between pixel distribution and brightness, color, and other data, it is converted into digital signals. These digital signals are then converted into corresponding formats and processed in a computer for analysis to obtain the required information, thereby achieving judgment of the target state. Then, the computer processes the digital video data and outputs it to the display device. In practical applications, this system has a high accuracy rate in detecting moving objects. The image system extracts the target features of the aforementioned signal through various operations and, based on the discrimination results, controls the movement of on-site equipment [18-20].

Machine vision technology mainly focuses on digital image processing, which involves converting various image signals into digital signals and processing them with computers. It requires more labor, but without corresponding intelligent devices for control, it leads to low production efficiency. Therefore, researching digital image processing technology and developing machine vision systems with intelligent features are of great significance for enhancing the competitiveness of enterprises and promoting social and economic development. Digital image processing technology, in a general sense, can be regarded as the collective term for various image processing techniques. It includes a series of operations completed by computers and other electronic devices, such as image acquisition, capture, encoding, storage, and transmission, image synthesis and generation, image display, drawing and output, image transformation, enhancement, and other functions, restoration and reconstruction, feature extraction and measurement, target detection, representation and description, correction of sequence images, image classification, representation and determination, etc.

The main work of this paper is to study the extraction method of markings on welds, using machine vision technology to process images, obtain the required self-image regions, and then mark the welds in the image regions. Finally, the data obtained from each algorithm is analyzed and compared. In practice, there are various factors that affect images. By using edge detection methods for evaluation, will there be precision errors? Based on this feature extraction, combined with image processing, the data accuracy rate is improved. The specific flowchart is shown as follows.



3.1 Image Preprocessing

Image processing includes image acquisition, image preprocessing, edge detection of the target, feature information extraction, etc. It can simulate the human visual process through a computer and implement automatic control. In this paper, mainly the relevant technical algorithms of weld seam marking are adopted, including image noise, regional filtering, edge detection of the target, etc.

Machine vision technology is centered on digital image processing, which is to convert various image signals into digital signals and process them with a computer. The most widely used technology in industrial control is computer image processing technology. Digital image processing technology, in a general sense, can be regarded as a collective term for various image processing techniques. It consists of a series of operations performed by electronic devices such as computers, such as image acquisition, acquisition, encoding, storage and transmission, comprehensive generation of images, image display, drawing and output, image transformation, enhancement, restoration and reconstruction, feature extraction and measurement, target detection, representation and description, correction of sequence images, classification, representation and recognition of images, etc.

3.1.1 Gray-scale Transformation

Gray-scale transformation mainly focuses on individual pixels. By changing the gray-scale range of the original image data, the quality of the image is enhanced, making it clearer and easier to recognize. In practical applications, attention should also be paid to possible problems at each stage to better utilize the machine vision system. Generally, after gray-scale transformation, the dynamic range of pixels increases, and the contrast of the image is expanded. Different types of gray-scale transformations can produce different effects. If the pixel value k at a certain image position in the source image is assumed to be transformed by the algorithm formula $F(k)$, then the pixel value at that position becomes H . Since there is a mapping relationship between the gray-scale images through the function $F(k)$, the formula after gray-scale transformation is the expansion of its mapping formula.

3.1.2 Binary Image

The common understanding is that a black-and-white image refers to a gray-scale image. In practical applications, in addition to gray-scale images, there is also a type of binary image. Strictly speaking, a binary image is a true black-and-white image. Since the gray-scale of a binary image can only reach between 0 and 255, 0 represents black and 255 represents white. This paper first introduces a new histogram equalization method based on the gray-scale space, which can adjust the brightness and

color information of the image according to actual needs. If the gray-scale value of a pixel in an image exceeds the set threshold, the pixel value in the image becomes 255; otherwise, it becomes 0.

3.1.3 Average Method

The basic concept of the average method is to convert the gray-scale value into the average value of R , G , and B . Eq. (1) is as follows:

$$R = G = B = (R + G + B) / 3 \quad (1)$$

This method is often used in scenarios where the contrast between light and dark in the image needs to be emphasized; the resulting image has a softer brightness but may weaken the color contrast.

3.1.4 Maximum-Minimum Average Method

The maximum-minimum average method is similar to the average method, which averages the maximum and minimum brightness values of the gray-scale image. The images generated by this method adjust the grayscale representation by combining the maximum and minimum brightness, which may result in detail loss due to the relatively high brightness.

3.2 Image Denoising

All the current digital images are noisy images, which means that the image data contains some useless and chaotic information as well as interference information. These noises are usually manifested as pixels or pixel blocks with strong visual effects. By using image filtering algorithms, the noise in the target image can be suppressed while retaining the feature information of the image. Generally, there are two types of filtering: linear and nonlinear. Mean filtering is linear, averaging all the pixel values in a certain area and giving the average value to the pixel at the center of the image. Nonlinear filtering is more difficult than linear filtering, as it requires calculating the maximum or minimum value of a certain range of pixels, and it is nonlinear. The formula for image filtering is as follows: (X represents the input image, i represents the horizontal coordinate, and j represents the vertical coordinate)

$$Y(i, j) = f[X(i-P, j-q), \dots, X(i, j), \dots, X(i+P, j+p)] \quad (2)$$

By applying this method to denoise the image before processing, not only can the quality of the image be significantly improved, but also the interference of useless information in data detection can be avoided.

3.2.1 Linear Filtering

Because the mapping function of linear filtering is linear, the convolution form is expressed as $Y = h \cdot X$, and the convolution kernel is h , so the formula 3 is as follows:

$$Y(i, j) = \sum_{m=-p}^p \sum_{n=-q}^q h(m, n) \cdot X(i + m, j + n) \quad (3)$$

This equation represents the convolution operation used in mean and Gaussian filters, which smooth the image and reduce noise before edge detection. Common linear filters include mean filtering and Gaussian filtering, etc. Mean filtering averages the pixel values in the target area and assigns the average value to the center pixel. Gaussian filtering is a method that averages all the pixel values in the image and then calculates the center point coordinates. Gaussian filtering refers to performing Gaussian weighting on the pixel values within the target range and then filtering the unknown pixel at the center. This method is suitable for images with small gray-scale changes or strong local contrast [21].

3.2.2 Nonlinear Filtering

Commonly used nonlinear filters include median filtering and bilateral filtering, etc. Each nonlinear filter does not have a specific form, so general nonlinear filtering takes the maximum or minimum value of the pixel values within a certain range and then performs filtering, replacing the pixel value at the center position. This method is suitable for images with small gray-scale changes or strong local contrast. Median filtering arranges the pixel values within the range in order and then performs filtering, replacing the pixel value at the center position with the median value.

After image denoising, some characteristics of the image may be obscured. If the edges of the image are blurred, it will cause the image to lose some characteristics, resulting in errors and missed detections in subsequent processing, and reducing the accuracy of the data. Therefore, to ensure the accuracy and effectiveness of subsequent data processing, effective image denoising must be performed to obtain more accurate data information. From the image processing results, it can be seen that the filtering algorithm produces different effects in the image, which may be similar to the original image or may have significant differences. Therefore, it is necessary to select the appropriate filtering method based on the characteristics of the specific image. In current image processing, choosing the appropriate algorithm based on the image situation will increase the expected results of image processing. For different feature data, choosing the appropriate filtering method is the greatest advantage of filtering.

3.3 Edge Detection

Edge detection is actually a filtering algorithm, and the difference from other filtering algorithms lies in the selection of the filter. The characteristics of the common filter are that the Gaussian filter uses the discretized Gaussian function to form a convolution kernel. Third, the Gaussian kernel operates on the target image to generate a grayscale matrix. Edge detection technology is widely used in computer vision, as it can clearly display the small structures and details on the surface of objects. The most widely used edge detection filters currently include Sobel, Prewitt, Roberts, and Canny operators, etc., to improve

detection accuracy. Targeted operators should be used for different image information. To correctly extract useful feature data, this paper mainly conducts comparative analysis based on different algorithms and collects and integrates data.

3.3.1 Edge Detection - Roberts Operator

Among the classic operators, the Roberts operator is the simplest edge detection operator. The Roberts operator uses the difference in certain areas of the image to search for edges and has greater superiority in locating edge positions compared to other operators. However, for images with high noise, the effect is poor, and the edge lines of the target image are not accurate. Due to its weak noise resistance, this algorithm is usually used for images with steep and low-noise edges. The basic image is $f(x, y)$, and the edge detection image of the Robert operator is $g(x, y)$ [22]. The algorithm 4 can be expressed as:

$$g(x, y) = \left\{ \begin{array}{l} [f(x, y) - f(x+1, y+1)]^2 + \\ + [f(x+1, y) - f(x, y+1)]^2 \end{array} \right\}^{0.5} \quad (4)$$

This operator highlights edges by measuring intensity differences along diagonal directions, but it is highly sensitive to noise.

3.3.2 Edge Detection with Prewitt Operator

Compared with the Robert operator, the Prewitt operator has stronger noise resistance and is thus less affected by waves. Essentially, it is a differential operator that uses the grayscale of pixels in the image within a region for differentiation. Therefore, the Prewitt operator is more suitable for images with high noise levels [23].

3.3.3 Edge Detection with Sobel Operator

The Sobel operator belongs to a class of discrete differentials and is composed of Gaussian smoothing and differential derivation. It is usually used to approximately calculate the brightness of an image. According to the target image, edge processing is performed on the region, and special points with a brightness level greater than a certain threshold in the region are marked. Edge detection technology is widely used in computer vision and can clearly display the fine structures and details on the surface of objects. Compared with the Prewitt operator, the Sobel operator pays more attention to the weights in the calculation. The influence on the target pixel varies with the distance from the neighboring points. The closer the better, the greater the influence on the target pixel. Thus, the edge contours of the image are marked.

3.3.4 Edge Detection with Canny Operator

The Canny operator was first invented by Australian computer scientist John Canny in 1986. Compared with other basic edge detection operators, it is one of the more advanced edge detection operators currently. The optimal edge is defined as the edge that the algorithm can mark

multiple times on the target image, and the marked edge can be closer to the actual edge in the image. The edge of the target can only be marked once, and there may be problems such as noise in the image not being marked as an edge.

When using the Canny operator for edge detection, first, Gaussian filtering is used to eliminate noise interference in the target image. Then, the target image is gradientized. Second, the non-maxima of the gradientized image are suppressed. Due to the interference of edges in the gradientized image, the non-maxima suppression method is used to search for the maximum value of the target region pixels. Finally, the purpose is achieved by using the double-threshold edge connection method and further verifying the existence of pseudo-edges.

4 COMPARISON AND ANALYSIS OF EXPERIMENTAL RESULTS

4.1 Construction of the Experimental Platform

The machine vision simulation based on the MATLAB platform can enable the computer to use machine vision for image acquisition, preprocessing, edge detection, etc., and the main function is to collect the data of various weld markings, and also optimize the characteristic defects of various weld images.

To ensure the scientific nature of the experimental results, we unified the parameters during the experiment, that is, the experiments were conducted under the same edge detection threshold and Gaussian filter standard deviation. Three typical welds were selected for the experiment, including three common types of welds: arc weld, butt weld, and fillet weld, which correspond to weld types I to III respectively.

For the evaluation of the weld extraction accuracy of the algorithm, there are currently two mainstream evaluation methods. The first one is to use visual inspection, presenting the experimental effect images to different evaluators, who then judge the quality of the experimental results. The best solution is ultimately determined through statistics. The other method is to use quantitative indicators, with many related indicators available. In this study, considering the characteristics of the research object, we selected four quantitative evaluation indicators: point sharpness, entropy, average gradient, and Quality Assessment of Blended Features.

Among them, point sharpness (PS) is an important indicator for measuring the clarity of an image. It assesses the sharpness of edge information by calculating the local contrast of each pixel in the image. Entropy (EN) represents the average amount of information contained in an image. The higher the entropy value, the more information it contains. Average gradient (AG), also known as clarity, reflects the contrast of fine details and texture changes in the image, and also indicates the clarity of the image. The higher the value, the better. Quality Assessment of Blended Features (QABF) is an indicator used to evaluate the effect of image fusion. It mainly measures the quality of feature retention in the fused image. This indicator analyzes the similarity of the fused image and the source image at the feature level to determine whether the key information of the original image is effectively retained after image fusion.

4.2 Comparison of Experimental Results

The weld type in Fig. 2 was detected, and the detection effect is shown in Fig. 3. Under the condition of ensuring the same experimental parameters, the Canny operator detects the most clear and complete weld seam information. The Sobel and Prewitt operators detect more weld seam information than the Roberts operator, but the information detected by all of them is incomplete. In the comparison of the four quantitative evaluation indicators, namely point sharpness, entropy, average gradient, and Quality Assessment of Blended Features, the Canny operator also demonstrated a significant performance advantage. For instance, in the point sharpness indicator, the performance of the Canny operator was 17 times that of the Roberts operator (Tab. 1).



Figure 2 Weld seam type I

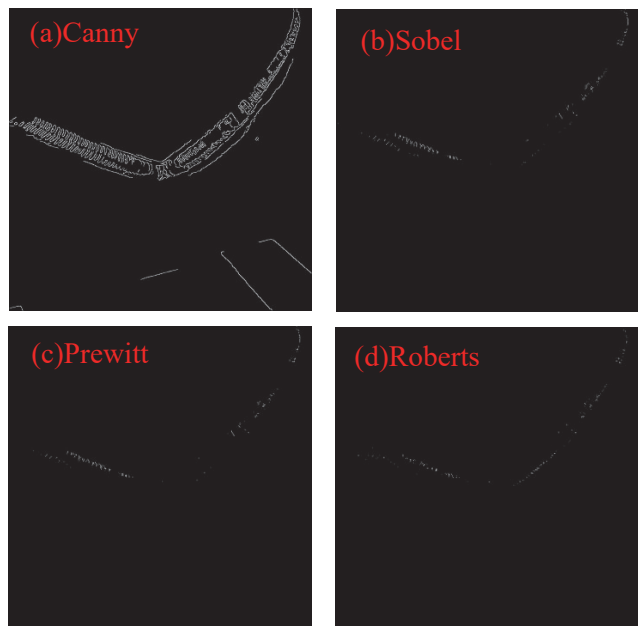


Figure 3 The detection effects of four edge detection operators on weld type I

Table 1 Comparison of detection effect indicators of four edge detection operators

Evaluation Index	PS	EN	AG	QABF
Canny	38.4055	0.6003	4.3872	0.0330
Sobel	3.4306	0.1166	0.3495	0.0074
Prewitt	2.5469	0.0942	0.2568	0.0053
Roberts	2.2527	0.0977	0.2357	0.0045



Figure 4 Weld seam type II

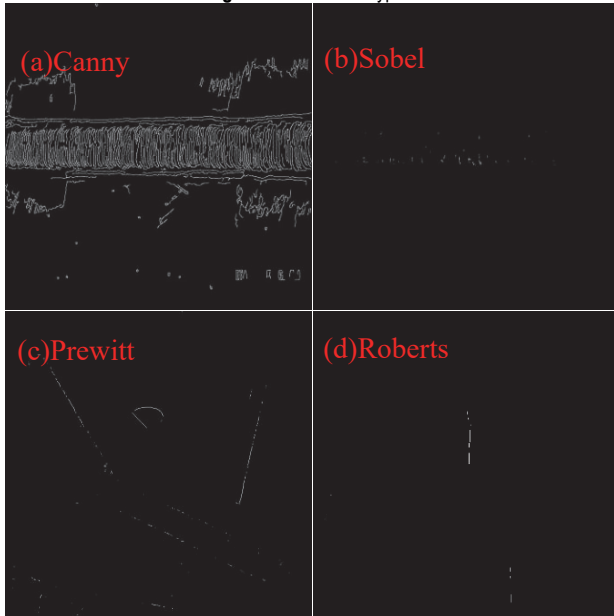


Figure 5 The detection effects of four edge detection operators on weld type II

Table 2 Comparison of detection effect indicators of four edge detection operators

Evaluation Index	PS	EN	AG	QABF
Canny	120.7326	1.3651	11.6192	0.0141
Sobel	1.4044	0.0605	0.1424	5.4952×10^{-4}
Prewitt	1.1732	0.0509	0.1185	4.2009×10^{-4}
Roberts	2.2432	0.0923	0.2357	0.0017

The weld type in Fig. 5 was detected, and the detection effect is shown in Fig. 6. Under the same experimental parameters, the weld features detected by Roberts, Prewitt and Sobel operators are all incomplete, but Prewitt is superior to Sobel operator, and the detection result of Roberts operator is the worst. In the comparison of the four quantitative evaluation indicators of point sharpness, entropy, average gradient and Quality Assessment of Blended Features, the performance advantage of Canny operator is also obvious (Tab. 2).



Figure 6 Weld seam type III

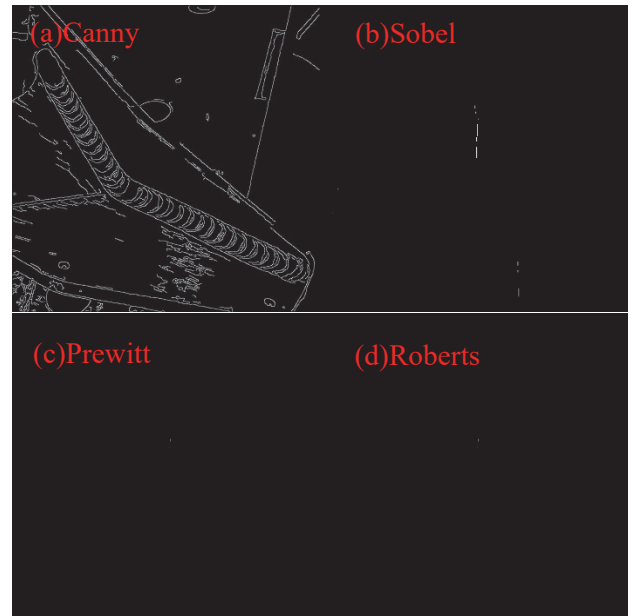


Figure 7 The detection effects of four edge detection operators on weld type III

Table 3 Comparison of detection effect indicators of four edge detection operators

Evaluation Index	PS	EN	AG	QABF
Canny	95.5220	1.4010	10.6957	0.0345
Sobel	5.6405	0.2087	0.6032	0.0075
Prewitt	4.5588	0.1774	0.4853	0.0060
Roberts	4.8554	0.2151	0.5250	0.0062

The weld type depicted in Fig. 7 was analyzed, and the detection outcomes are presented in Fig. 8. The detection result of the Canny operator is the least affected, and the image is very clear. The weld contour is completely marked, achieving the ideal image result. The weld features detected by the Roberts, Prewitt, and Sobel operators are all incomplete. In the comparison of the four quantitative evaluation indicators of point sharpness, entropy, average gradient, and Quality Assessment of Blended Features, the Canny operator also shows obvious performance advantages (Tab. 3).

To further verify the advantages of the Canny operator in weld defect detection, this study selected welding defect images for further research. Common welding defects include porosity, slag inclusion, incomplete penetration, incomplete fusion, cracks, pits, undercut, and weld spurs, etc. Among these defects, welding crack defects are typical

edge contour detection cases. As shown in Fig. 8, there is a crack defect in the weld seam, which is the position indicated by the red box in the figure. Now, four operators are used respectively to mark the welding crack defect.



Figure 8 Welding crack

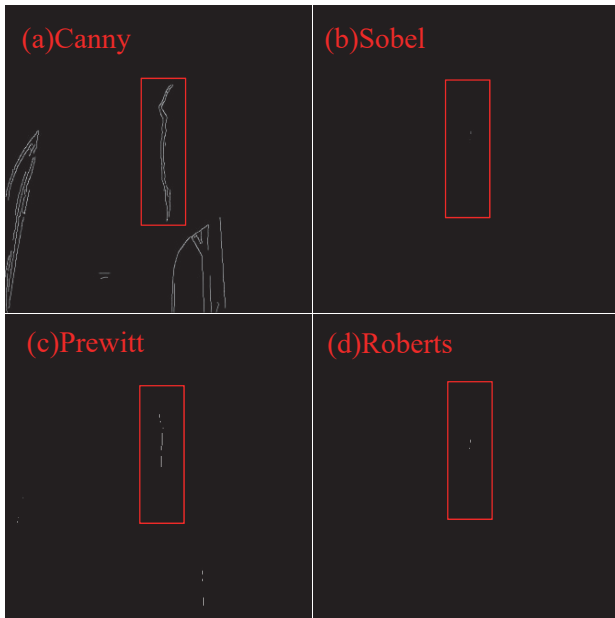


Figure 9 Welding crack detection effect

Table 4 Comparison of detection effect indicators of four edge detection operators

Evaluation Index	PS	EN	AG	QABF
Canny	17.9042	0.3314	1.7096	0.0110
Sobel	0.0710	0.0054	0.0073	3.6724×10^{-4}
Prewitt	0.0710	0.0054	0.0073	3.6724×10^{-4}
Roberts	0.7147	0.0240	0.0623	0.0035

As can be seen from the welding crack detection results in Fig. 9, under the same experimental parameters, the Canny operator can accurately, clearly and completely mark the location of the welding cracks; although the Prewitts operator cannot completely mark the location of the welding cracks, its marking effect is better than that of the Sobel and Roberts operators, and the detection effect of the Roberts operator is the worst. In terms of the relevant indicators of image detection, the Canny operator also has obvious advantages (Tab. 4).

4.3 Analysis of Experimental Results

In terms of the overall experimental data, the Canny operator's detection is the most stable and the image is very clear. Although the operator itself has a high level of anti-interference, there is still a certain amount of noise in the image. The Roberts operator detects images with less noise, but it has the least weld feature information. The Prewitt operator has a better detection effect than the Roberts and Sobel operators, but the detected weld features are still incomplete. By comparing several commonly used algorithms, after this test, the Canny operator is the best choice in most cases. Although the Canny operator tends to detect features that do not belong to the feature area during detection, thus showing the characteristic of large image noise, this kind of noise can actually be solved through some preprocessing methods, such as creating the detection area as a region of interest (ROI), which can reduce the detection area of the image and avoid non-feature areas from being detected, thereby reducing the noise in the Canny operator's image detection. For a specific summary, see Tab. 5.

Table 5 Summary of edge detection operator detection effects

Evaluation Index	Strengths	Weaknesses	Suitable Conditions
Canny	Bestrobustnes, clear edges	The image has a lot of noise.	The image has low noise.
Sobel	The image has low noise.	The edges of the detected image are incomplete.	
Prewitt	The image has low noise.	The edges of the detected image are incomplete.	
Roberts	The image has low noise.	The edges of the detected image are incomplete.	

5 CONCLUSION

This paper presents simulation experiments on weld marking based on machine vision. By understanding various operator algorithms, constructing the MATLAB platform, writing the algorithm code for the platform, and conducting in-depth research using MATLAB simulations, it integrates the characteristics of machine vision with weld marking technology. The test data obtained from detecting and marking various weld seam images on the completed platform have achieved satisfactory results. The specific work is as follows: (1) In weld marking, interference from different factors is unavoidable. For high-noise images, noise reduction preprocessing is applied to optimize image quality and minimize interference effects. For low-noise images, a method considering noise pixel values is adopted to enhance the image area. Appropriate measures are implemented to address the interference caused by different factors and improve the quality of experimental data. (2) An analysis of weld marking images is conducted using edge detection algorithms such as Sobel, Roberts, Prewitt, and Canny. A comparative study is performed, and the most suitable method for optimizing image quality is selected. The results demonstrate that the Canny operator provides the best balance of robustness and clarity, making it suitable for practical industrial weld seam inspection systems. Future research will focus on integrating edge detection with lightweight neural models to combine the

simplicity of traditional methods with the adaptability of AI approaches.

6 REFERENCES

- [1] Li, J., Lai, C., Wang, Y., Luo, A., & Yuan, X. (2024). SpectrumVA: Visual Analysis of Astronomical Spectra for Facilitating Classification Inspection. *IEEE Transactions on Visualization and Computer Graphics*, 30(8), 5386-5403. <https://doi.org/10.1109/TVCG.2023.3294958>
- [2] Bi, Q. L., Lai, M. L., Chen, K., Liu, J. M., Tang, H. L., Teng, X. B., & Guo, Y. Y. (2023). Spatial position recognition method of semi-transparent and flexible workpieces: A machine vision based on red light assisted. *Advances in Production Engineering & Management*, 18(1), 49-65. <https://doi.org/10.14743/apem2023.1456>
- [3] Ly Duc, M., Hlavaty, L., Bilik, P., & Martinek, R. (2023). Enhancing manufacturing excellence with Lean Six Sigma and zero defects based on Industry 4.0. *Advances in Production Engineering & Management*, 18(1), 32-48. <https://doi.org/10.14743/apem2023.1455>
- [4] Si, Q. M., Li, J. Y., Guo, X. Y., Wang, H., & Liu, C. Y. (2024). Simulation of the Evacuation Strategy for an Air-Rail Intermodal Hub Station. *International Journal of Simulation Modelling*, 23(3), 483-494. <https://doi.org/10.2507/IJSIMM23-3-696>
- [5] Zhang, B., Wang, X., Cui, J., Wu, J., Xiong, Z., Zhang, W., & Yu, X. (2024). Enhancing Weld Inspection Through Comparative Analysis of Traditional Algorithms and Deep Learning Approaches. *Journal of Nondestructive Evaluation*, 43(2), 38. <https://doi.org/10.1007/s10921-024-01047-y>
- [6] Liang, H., Qi, L., & Liu, X. (2024). Modeling and optimization of robot welding process parameters based on improved SVM-PSO. *The International Journal of Advanced Manufacturing Technology*, 133(5-6), 2595-2605. <https://doi.org/10.1007/s00170-024-13800-8>
- [7] Choi, K.-H., & Ha, J.-E. (2023). An Adaptive Threshold for the Canny Edge With Actor-Critic Algorithm. *IEEE Access*, 11, 67058-67069. <https://doi.org/10.1109/ACCESS.2023.3291593>
- [8] Min, X., Zou, Y., & Zhang, C. (2010). Research on post-welding quality visual inspection system of tailored blanks laser welding. *2010 2nd International Asia Conference on Informatics in Control, Automation and Robotics (CAR 2010)*, 349-353. <https://doi.org/10.1109/CAR.2010.5456529>
- [9] Society, A. W., Wang, S., Chen, J., Xia, C., Wu, C., Zhang, W., & Li, R. (2023). Weld Geometry Prediction Based on Binocular Vision and Deep Learning. *Welding Journal*, 102(8), 177-190. <https://doi.org/10.29391/2023.102.014>
- [10] Zeng, B., Wang, Y., Ye, L., & Yang, S. (2024). Using fiber optic sensors to monitor the quality of resistance spot welding joints. *Science and Technology of Welding and Joining*, 29(5-6), 309-318. <https://doi.org/10.1177/13621718241272122>
- [11] Kim, C., Shim, Y.-D., Kim, J., Gu, J., & Lee, E.-H. (2024). Inspection of welded quality in thermoplastic welding using ultrasonics under different temperature conditions. *Journal of Mechanical Science and Technology*, 38(10), 5209-5218. <https://doi.org/10.1007/s12206-024-2304-1>
- [12] Germano, E., Tabatabaeipour, M., Mohseni, E., Lines, D., MacLeod, C. N., Lam, K.-H., Hughes, D., Trodden, H., & Gachagan, A. (2025). Application of Golay-based total focusing method using a high-frequency, lead-free, flexible ultrasonic array for inspection of thick non-planar industrial components. *NDT & E International*, 150, 103282. <https://doi.org/10.1016/j.ndteint.2024.103282>
- [13] Zhai, M., Locquet, A., & Citrin, D. S. (2024). Terahertz nondestructive layer thickness measurement and delamination characterization of GFRP laminates. *NDT & E International*, 146, 103170. <https://doi.org/10.1016/j.ndteint.2024.103170>
- [14] Wu, Z., Wang, Y., Xie, H., Feng, M., Wu, H., Ding, C., & Mian, A. (2024). A Systematic Point Cloud Edge Detection Framework for Automatic Aircraft Skin Milling. *IEEE Transactions on Industrial Informatics*, 20(1), 560-572. <https://doi.org/10.1109/TII.2023.3268404>
- [15] Zhou, W., Zhao, L., Huang, H., & Wang, C. (2025). Data-Efficient Object Detection on Construction Sites Using Reweighting Mechanism and Cross-Batch Contrastive Learning. *IEEE Transactions on Industrial Informatics*, 21(8), 6028-6037. <https://doi.org/10.1109/TII.2025.3558311>
- [16] Lan, Y.-S., Wang, Q., Yang, J.-G., Meng, X.-Q., Yang, Y. (2025). Enhanced Lane Recognition for Automated Warning Sign Placement Using Canny Edge Detection. *Tehnicki Vjesnik - Technical Gazette*, 32(4), 1529-1538. <https://doi.org/10.17559/TV-20230918000947>
- [17] Wu, Y., Shi, J., Xiao, B., Zhang, H., Ma, W., Wang, Y., Liu, B. (2025). Efficient Detection and Measurements of Bridge Crack Widths Based on Streamlined Convolutional Neural Network. *Tehnicki Vjesnik - Technical Gazette*, 32(1), 123-131. <https://doi.org/10.17559/TV-20240519001615>
- [18] Li, Y., Yu, B., Wang, B., Lee, T. H., & Banu, M. (2020). Online quality inspection of ultrasonic composite welding by combining artificial intelligence technologies with welding process signatures. *Materials & Design*, 194, 108912. <https://doi.org/10.1016/j.matdes.2020.108912>
- [19] Liang, H., Qi, L., & Liu, X. (2024). Modeling and optimization of robot welding process parameters based on improved SVM-PSO. *The International Journal of Advanced Manufacturing Technology*, 133(5-6), 2595-2605. <https://doi.org/10.1007/s00170-024-13800-8>
- [20] Chen, R., Hu, P., Gui, X., & Hua, L. (2024). An on-line weld inspection method for underwater offshore structure based on an improved deep convolutional network. *Nondestructive Testing and Evaluation*, 40(1), 289-308. <https://doi.org/10.1080/10589759.2024.2319261>
- [21] Kikuchi, T., Takabatake, R., Katayama, K., Ikenoue, H., & Nakamura, D. (2024). Joint quality assessment by machine learning using characterized surface thermal radiation images of laser welding process. *High-Power Laser Materials Processing: Applications, Diagnostics, and Systems XIII*, 22. <https://doi.org/10.1117/12.3000891>
- [22] Huang, H., Peng, X., Hu, X., & Ou, W. (2024). Efficient Object Detection and Recognition of Body Welding Studs Based on Improved YOLOv7. *IEEE Access*, 12, 41531-41541. <https://doi.org/10.1109/ACCESS.2024.3376473>
- [23] Liao, B., Zuo, H., Yu, Y., & Li, Y. (2024). GraphMriNet: a few-shot brain tumor MRI image classification model based on Prewitt operator and graph isomorphic network. *Complex & Intelligent Systems*, 10(5), 6917-6930. <https://doi.org/10.1007/s40747-024-01530-z>

Contact information:

Chenlei ZHAO, Lecturer
Geely University of China,
Chengdu 641423, China
E-mail: zhaochenlei@stu.xhu.edu.cn

Dong WU, Lecturer
Geely University of China,
Chengdu 641423, China
E-mail: 447325098@qq.com

Lin XI, Lecturer
Geely University of China,
Chengdu 641423, China
E-mail: lishang_1880@163.com

Lihong GUO, Associate professor
(Corresponding author)
Chengdu Jincheng College,
Chengdu 611731, China
E-mail: guo_lihong123@126.com

Shenghong WU, Lecturer
Sichuan Technology & Business College,
Chengdu 611830, China
E-mail: 1529432209@qq.com

Xiao LUO, Assistant Researcher
Geely University of China,
Chengdu 641423, China
E-mail: 535292271@qq.com

Shunyang HU, M.S. Student
Hosei University,
Tokyo 1638001, Japan
E-mail: kojunyou@gmail.com

Yiran DING, B.E. Student
Geely University of China,
Chengdu 641423, China
E-mail: 3180900037@qq.com